

**SEISMIC VELOCITY ESTIMATION IN THE MIDDLE EAST FROM MULTIPLE WAVEFORM
FUNCTIONALS: P & S RECEIVER FUNCTIONS, WAVEFORM FITTING,
AND SURFACE WAVE DISPERSION**

Mrinal K. Sen¹, Jay Pulliam², Utpal Dutta³, Ranjana Ghosh¹, Rengin Gök⁴, and Michael Pasyanos⁴

The University of Texas at Austin¹, Baylor University², University of Alaska, Anchorage³,
and Lawrence Livermore National Laboratory⁴

Sponsored by the National Nuclear Security Administration

Award Nos. DE-AC52-09NA29327 and DE-AC52-07NA27344
Proposal No. BAA09-58

ABSTRACT

We demonstrated that SPL waveform data, together with associated phases, are able to constrain crustal and upper mantle seismic wave velocity structures. Forward modeling is done using a reflectivity algorithm and optimization is carried out using an algorithm called very fast simulated annealing (VFSA). The code runs efficiently on multiple processors using MPI routines. The advantages of VFSA include

- It is derivative free and therefore, the objective function can be changed to include disparate datasets without any changes in the algorithm, and
- Models from multiple VFSA runs can be used to obtain estimates of uncertainty.

We are currently developing a new algorithm to derive crustal velocity structure by modeling SPL wavetrains, surface wave dispersion and receiver function data from collocated source-receiver pairs. Optimization is done using a three part objective function given by

$$Error = a_1 \left\| \mathbf{d}_{SPL}^{obs} - \mathbf{d}_{SPL}^{syn} \right\|_p + a_2 \left\| \mathbf{d}_{dispersion}^{obs} - \mathbf{d}_{dispersion}^{syn} \right\|_p + a_3 \left\| \mathbf{d}_{receiverfunction}^{obs} - \mathbf{d}_{receiverfunction}^{syn} \right\|_p, \quad (1)$$

where a_1 , a_2 and a_3 are the relative weights of different data and p is the norm used to measure data misfit. The algorithm is very general in that the weights can change with iteration and p can take different values for the three different parts of the objective function. Note that the same model is used to compute synthetic SPL waveform, surface waves and receiver function data.

Since SPL calculation takes the longest, the reflectivity calculation is distributed over ray-parameters using MPI calls. On the other hand, one node each is allocated to compute surface wave dispersion and receiver function, resulting in efficient load balancing. The following issues are currently being investigated:

- Types of objective functions to be used,
- Values of weights assigned to different data types,
- Influence of different datasets on the derived model estimates.

The algorithm will be applied to data recorded at broadband seismic stations in the Middle East, an area of strategic interest and one for which there exist previous results of surface wave dispersion and receiver function modeling. We have developed statistical tools, including estimates of the Posterior Probability Density (PPD) functions and parameter correlation matrices, which allow us to evaluate the uniqueness and physical feasibility of resulting models. These tools will allow us to evaluate the relative strength of constraints placed on model parameters by each type of data in addition to the portions of the model that are well- or poorly constrained.

OBJECTIVES

One goal of the BAA to which this proposal responds is to develop optimal procedures for the use of multiple datasets. Due to the inherent variability, inconsistency, and peculiarities of disparate datasets and the well-known nonlinearity and non-uniqueness associated with geophysical modeling, such procedures must include methods for evaluating the performance and contribution of each dataset to the final results.

Our approach makes use of quantitative assessment tools and a well-developed Bayesian approach to explore and evaluate each step of the modeling process, rather than to simply toss all constraints into a simultaneous fitting procedure to find the single solution that satisfies particular criteria. The procedure we propose, best characterized as velocity analysis via optimization, is analogous to velocity analysis in exploration seismology, rather than “inversion”. It will provide quantitative error measures of structural parameter estimates that can then be translated to earthquake location errors, and thus guide seismologists toward the most effective and efficient ways to improve model reliability.

RESEARCH ACCOMPLISHED

We have made substantial progress in developing, testing, and applying the method for waveform modeling via global optimization described above (Gangopadhyay et al., 2007; Pulliam and Sen, 2005; Pulliam et al., 2006). Earlier we developed, with Lian-She Zhao and Cliff Frohlich, a VFSA-based inversion algorithm for P-wave receiver functions (Zhao and Frohlich, 1996; Zhao et al., 1996). Additional tools we developed include a fast, parallelized reflectivity code that incorporates anisotropic model parameters, additional global optimization methods based upon genetic algorithms, and numerous imaging algorithms.

Specifically with regard to waveform modeling: We developed a code that computes synthetic seismograms with a parallelized reflectivity method and fits the observed waveforms by global optimization. Our method also computes the Posterior Probability Density (PPD) function and correlation matrix, to evaluate the uniqueness of the resulting models, and the trade-offs between individual model parameters therein. We applied the code to determine the crust and upper mantle structure beneath permanent broadband seismic stations in Africa using teleseismic earthquakes (M 5.5-7.0 and 200-800 km focal depth) recorded at these stations. We modeled the S, SP, SsPmP, and shear-coupled PL waves from these earthquakes and our P- and S-wave velocity models compare well with, and in some cases improve upon the models obtained from other existing methods. We obtained P- and S-wave velocities simultaneously and our use of the shear-coupled PL phase wherever available improved constraints on the models of the lower crust and upper mantle (Gangopadhyay et al., 2007).

During the past year, we have accomplished the following tasks listed below. Later we describe these in detail.

1. testing of waveform, surface wave dispersion and receiver function modeling codes using identical inputs,
2. development of a joint inversion code using all three different types of data sets,
3. extensive testing of objective functions appropriate for each data set,
4. efficient parallelization of the joint inversion code,
5. extensive testing with synthetic data, and
6. preliminary tests with a data set from the middle east.

Joint Modeling of Multiple Datasets

There are several advantages to jointly modeling multiple datasets. First, each data functional has unique sensitivities to Earth structure. For example, receiver functions are primarily sensitive to shear wave velocity contrasts and vertical traveltimes while surface wave dispersion measurements are sensitive to vertical shear wave velocity averages (Julia et al., 2000). Full waveform modeling of S, Sp, SsPmP phases, in contrast, are more sensitive to compressional wave velocity contrasts and vertical traveltimes; adding SPL to the modeling improves sensitivity to the uppermost mantle shear wave structure and to velocity contrasts across the Moho (Gangopadhyay et al., 2007). The amplitudes and signal-to-noise characteristics of waves that produce these data functionals depend on several factors, including epicentral distance, event focal depth, fault mechanism and radiation patterns, source time function, properties of the intervening Earth structure (including attenuation, low velocity zones, velocities, heterogeneity, and anisotropy), and characteristics of the recording seismometer. Since regions of high seismicity are highly restricted, many stations are not well situated to record appropriate events. An algorithm that incorporates multiple data types is more widely applicable than one that relies solely on a single type.

However, with these advantages come some disadvantages. For example, combining disparate data types requires great care in their treatment and assessment (Roy et al., 2005). Benefits of additional data may be null if the method used to model them preferentially fits one type. Or, worse, minimizing an inappropriate criterion in conjunction with

incompatible data may “split the difference” between them to choose a model that is wholly inaccurate and inappropriate for its intended purpose. If the model is to be used for regional or local earthquake locations, for example, it would be a mistake to rely on the best fit to surface wave dispersion. The judgment and experience of seismologists who keep a clear eye on their goal is critical, and this experience must be combined with rigor in the computational modeling. This experience and judgment can be incorporated after the fact, as is sometimes the case with, for example, the smoothing applied to 3D tomographic models but it is usually better to acknowledge the “prior” explicitly at the outset. This is one advantage of the Bayesian approach that we propose here. While priors are sometimes referred to pejoratively as “bias”, their explicit statement during the formulation of the modeling algorithm forestalls serious criticism and enables a clear, quantitative discussion of “bias”.

Next, as a general rule of thumb, a greater number of data functionals incorporated into modeling will result in a broader range of model parameter sensitivities, and it will be less likely that a linear inversion approach will be adequate. This is unfortunate because linear approaches are much more tractable and straightforward than nonlinear methods. But only a broad search of the model space will demonstrate whether a linear approach is valid. Non-linear global optimization algorithms require no change in the algorithm to include multi-part objective function with different norms. A variety of methods for nonlinear inversion are now available and the only real cost for conducting a thorough search and finding the single best-fitting model is in computational effort and complexity. The downside is that theoretically exact methods for assessing model uncertainties and model reliability are not generally tractable, and approximate methods result in significantly greater cost and complexity than is required to find the best-fitting model alone. Nevertheless, our previous work has demonstrated that useful methods are indeed tractable, and the method we propose will add only marginal increases in computation time.

While surface wave dispersion and receiver functions have been modeled jointly (Ammon et al., 2005; Ammon et al., 2004; Cakir and Erduran, 2004; Chang et al., 2004; Dugda and Nyblade, 2006; Herrmann et al., 2001; Julia et al., 2000; Julia et al., 2005; Lawrence and Wiens, 2004; Ozalaybey et al., 1997; Tkalcic et al., 2006), no study has, to our knowledge, incorporated waveform constraints such as S, Sp, SsPmP, and Shear-coupled PL. Further, none has conducted a thorough, nonlinear assessment of the constraints provided by each functional.

Multi-Objective Optimization for Multiple Datasets

The primary goal of our current project is to develop a tool for estimating crustal structure that can explain surface wave dispersion, receiver function and full waveform modeling. Thus our optimization algorithm is expected to minimize misfit of each of the datasets using three different objective or cost functions. The process of optimizing systematically and simultaneously a collection of objective functions is called multiobjective optimization (MOO) or vector optimization. The general MOO is posed as follows:

$$\underset{\mathbf{m}}{\text{Minimize}} \ F(\mathbf{m}) = [F_1(\mathbf{m}), F_2(\mathbf{m}), \dots, F_k(\mathbf{m})]^T, \quad (2)$$

where \mathbf{m} is the model vector, and k is the number of objective functions. The objective function is minimized subject to some constraints. In our application, we use standard constraints such as bounds and negativity.

Contrary to single-objective optimization, an MOO may be considered more of a concept than a definition. Typically, with noisy data there is no single global solution and it is often necessary to determine a set of points that all fit a predetermined definition for an optimum. This is commonly done using what is known as Pareto optimality (Pareto 1906) defined as follows.

Definition: A model \mathbf{m}^* belonging in the model space is said to be Pareto optimal if and only if there does not exist any other model \mathbf{m} in the model space such that $F(\mathbf{m}) \leq F(\mathbf{m}^*)$, and $F_i(\mathbf{m}) < F_i(\mathbf{m}^*)$ for at least one function.

We often use a *Global criterion* in search for models belonging to Pareto set, which is a scalar function that mathematically combines multiple objective functions; it may or may not involve preference of one or the other.

Objective Function

We use the following objective function which outputs a single scalar value.

$$\text{Error} = a_1 \left\| \mathbf{d}_{SPL}^{obs} - \mathbf{d}_{SPL}^{syn} \right\|_p + a_2 \left\| \mathbf{d}_{dispersion}^{obs} - \mathbf{d}_{dispersion}^{syn} \right\|_p + a_3 \left\| \mathbf{d}_{receiverfunction}^{obs} - \mathbf{d}_{receiverfunction}^{syn} \right\|_p. \quad (3)$$

This general objective function allows for different measures of error and different weights to the datasets. There are at least three fundamental issues that we need to address:

1. What measures of error do we use? Can they be different for different datasets?
2. Can we use simple differences?
3. How do we choose the three weights?

Question (3) does not generally have a straightforward answer. The weights have to be determined by trial and error. One important consideration in defining the global objective function for MOO is to ascertain that no individual objective function introduces more impact than the others unless so desired. To address this, we use the following normalized objective function defined in Sen and Stoffa (1995)

$$Error = 1 - \frac{2 \sum |d_{obs}^i - d_{syn}^i|^\alpha}{\sum |d_{obs}^i + d_{syn}^i|^\alpha + \sum |d_{obs}^i - d_{syn}^i|^\alpha}, \quad (4)$$

where the sum is taken over all the data points and the parameter α is equivalent to norm.

Initially we chose $\alpha=1$ for all three objective functions. Note that the SPL and receiver function make use of waveform data while the dispersion curve is fairly simple. The objective function corresponding to the surface wave dispersion is smoothly varying and therefore, we chose $\alpha=0.5$ to introduce more sensitivity. With these choices of α values and normalized objective functions as defined in the above equation, we employ equal weights to all three parts of the objective function.

There are several advantages to jointly modeling multiple datasets. First, each data functional has unique sensitivities to Earth structure. For example, receiver functions are primarily sensitive to shear wave velocity contrasts and vertical traveltimes while surface wave dispersion measurements are sensitive to vertical shear wave velocity averages (Julia et al., 2000). Full waveform modeling of S, Sp, SsPmP phases, in contrast, are more sensitive compressional wave velocity contrasts and vertical traveltimes; adding SPL to the modeling improves sensitivity to the uppermost mantle shear wave structure and to velocity contrasts across the Moho (Gangopadhyay et al., 2007). Mutually satisfying constraints imposed by the three datasets may constrain a larger subset of model parameters than a single set alone, resulting in a single model that better represents the true structure.

Optimization and Parallelization

Having defined the objective function, we employ VFSA for optimization (Pulliam and Sen, 2005; Sen and Stoffa 1995). Note that VFSA causes no difficulties since we do not require computing derivatives. As used in Pulliam and Sen (2005), we use a parallel optimization code for MOO as well. Note that the most expensive computation element is that of SPL waveform by the reflectivity method and therefore, the reflectivity computation is distributed over multiple nodes. Since surface wave dispersion and receiver function computations are fairly fast, we distribute those to one node each and thus achieve reasonable load balancing.

Results from a Synthetic Experiment

We generated synthetic S-waveform for three component seismograms, surface wave dispersion and receiver function for a simple six layer model. This dataset is then used as observation for optimization. Our model's search parameters are V_p , V_s , and layer thickness for the six layers. We use search bounds for the three model parameters, as shown in Fig 1(a). Figures 1, 2, and 3 show results from our inversion experiments using three different combination of weights, namely, (1) receiver function 0, dispersion 0, SPL 1; (2) receiver function 0, dispersion 1, SPL 1, and (3) receiver function 1, dispersion 0, SPL 1.

Thus Figure 3 corresponds to the case where all three datasets are weighed equally. The results show a mean model and posterior variances corresponding to different model parameters (see Pulliam and Sen 2005 for more details on this). Note that we run multiple VFSA with different starting models and use all the models to characterize uncertainty. In other words, we attempt to sample many models from the Pareto set. The impact of different weights is fairly obvious in the three figures. It seems SPL data has the most impact; by setting SPL=1 and the other two to zeros, we are able to obtain reasonable fit of surface wave dispersion and receiver function. When all the weights are set equal to one, we are able to match all three datasets and reproduce the model fairly well.

CONCLUSIONS AND RECOMMENDATIONS

We have developed a parallel VFSA based multi-objective optimization code that can be used to obtain crustal velocity structures by modeling SPL waveform, receiver function and surface wave dispersion data. The code has been tested successfully with a simple synthetic example. We will continue to test our code using more realistic synthetics and will then apply extensively to several datasets from the Middle East.

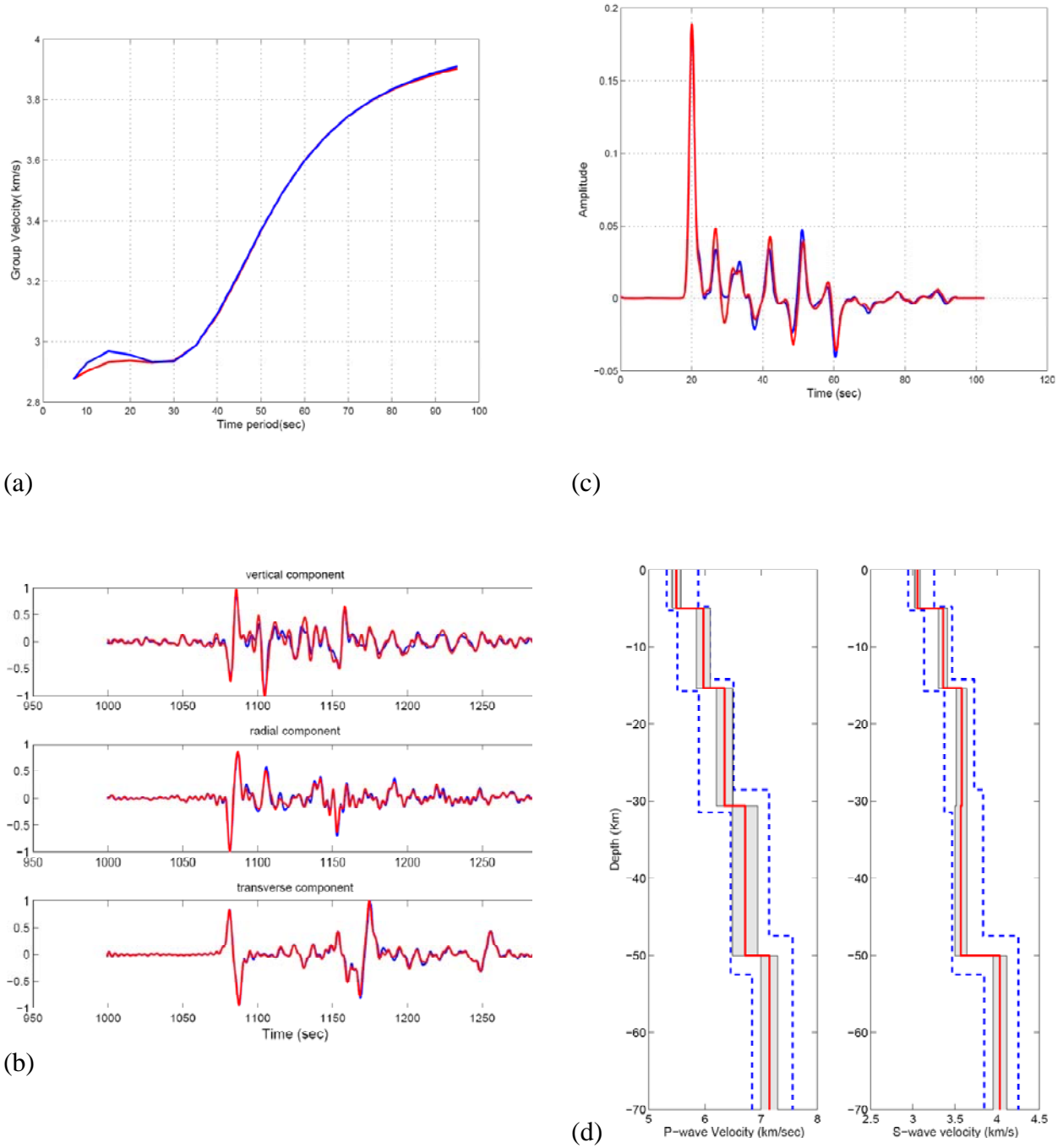


Figure 1. Results from joint inversion code: the weight for SPL data was set equal to one; the other two weights are zero. (a) surface wave dispersion, (b) SPL waveforms, (c) receiver function, (d) model fit. In figures (a)-(c), blue is the observed data and red the synthetic data. In figure (d), blue dotted lines are the model bounds; mean estimated model is the red line and the grey area is the uncertainty in the estimated model.

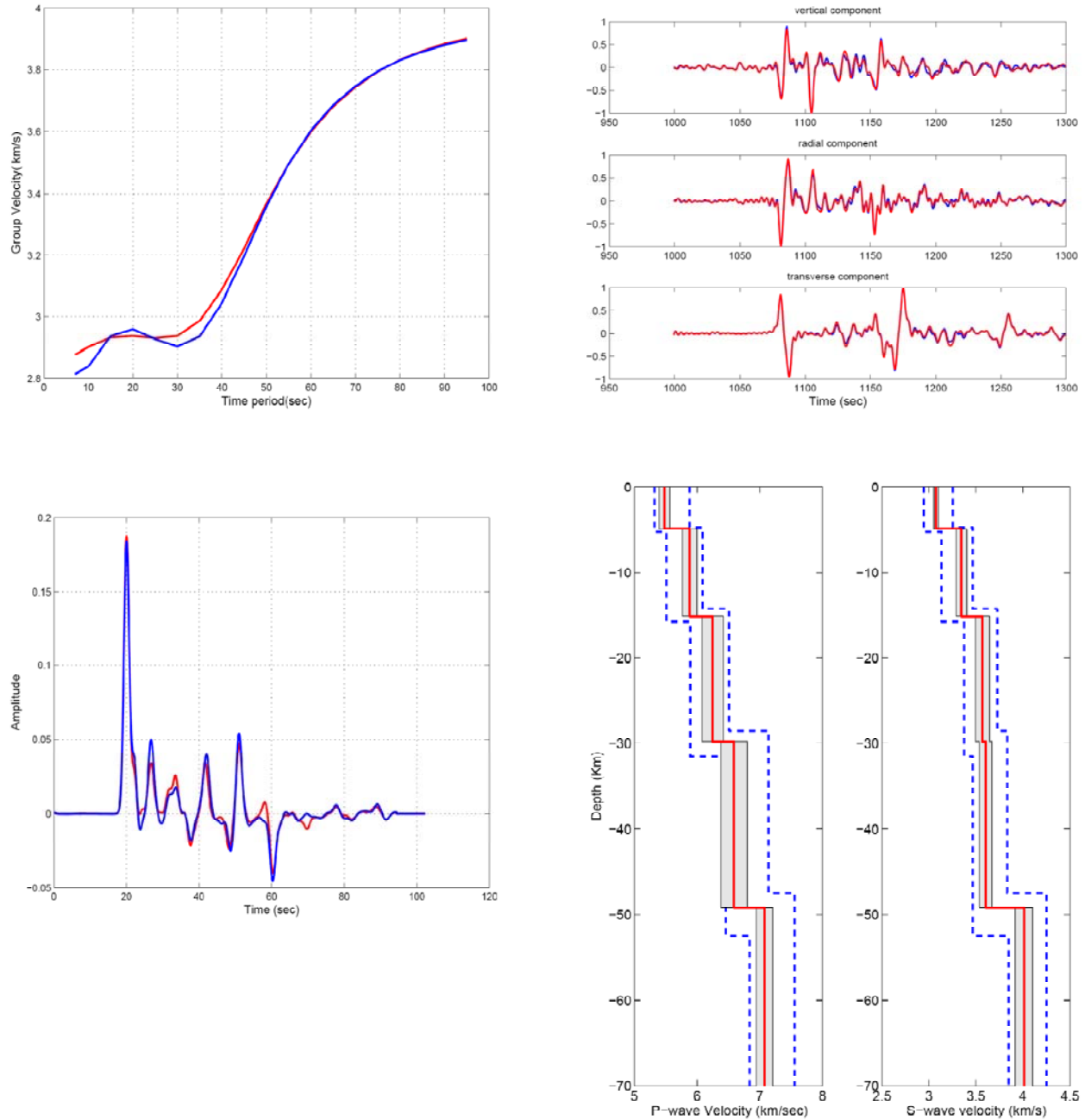


Figure 2. Results from joint inversion code: the weights for SPL and receiver function data were set equal to one only. (a) surface wave dispersion, (b) SPL waveforms, (c) receiver function, (d) model fit. In Figures (a)-(c), blue is the observed data and red the synthetic data. In Figure (d), blue dotted lines are the model bounds; mean estimated model is the red line and the grey area is the uncertainty in the estimated model.

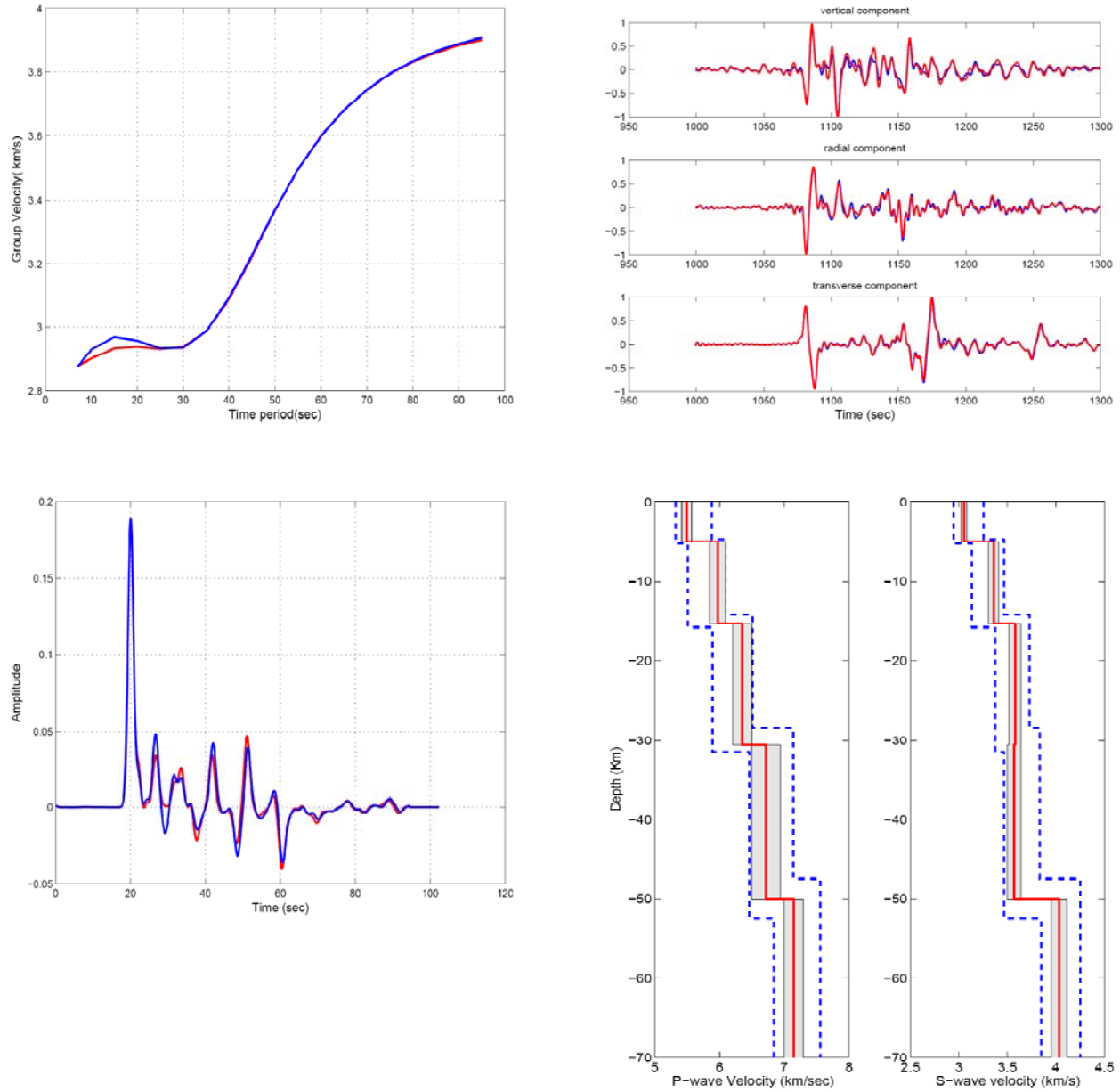


Figure 3. Results from joint inversion code: all three weights were set equal to one. (a) surface wave dispersion, (b) SPL waveforms, (c) receiver function, (d) model fit. In Figures (a)-(c), blue is the observed data and red the synthetic data. In Figure (d), blue dotted lines are the model bounds; mean estimated model is the red line and the grey area is the uncertainty in the estimated model.

REFERENCES

- Ammon, C.J., M. Kosarian, R. Herrmann, M. Payanos, W. Walter, W. Sevilla, and G. Randall (2005). Simultaneous Inversion of Receiver Functions and Surface-Wave Dispersion Measurements for Lithospheric Structure Beneath Asia and North Africa, in *Proceedings of the 27th Seismic Research Review: Ground-Based Nuclear Explosion Monitoring Technologies*, LA-UR-05-6407, Vol. 1, pp. 3–12.
- Ammon, C.J., M. Kosarian, R. Herrmann, M. Payanos, W. Walter, and H. Tkalcic (2004). Simultaneous Inversion of Receiver Functions, Multi-mode Dispersion, and Travel-time Tomography for Lithospheric Structure Beneath the Middle East and North Africa, in *Proceedings of the 26th Seismic Research Review—Trends in Nuclear Explosion Monitoring*, LA-UR-04-5801, Vol. 1, pp. 17–28.
- Cakir, O. and Erduran, M. (2004). Constraining crustal and uppermost mantle structure beneath station TBZ (Trabzon, Turkey) by receiver function and dispersion analyses. *Geophys. J. Int.*, 158(3): 955–971.
- Chang, S.-J., Baag, C.-E. and Langston, C. (2004). Joint analysis of teleseismic receiver functions and surface wave dispersion using the genetic algorithm. *Bull. Seismol. Soc. Am.* 94(2): 691–704.
- Dugda, M. and Nyblade, A. A. (2006). New constraints on crustal structure in eastern Afar from the analysis of receiver functions and surface wave dispersion in Djibouti. *Geological Society of London Special Publications*, 259: 239–251.
- Gangopadhyay, A., Pulliam, J. and Sen, M. K. (2007). Waveform Modeling of Teleseismic S, SP, SsPmP, and Shear-Coupled PL Waves for Crust and Upper Mantle Velocity Structure Beneath Africa. *Geophys. J. Int.*, 170: 1210–1226.
- Herrmann, R. B., Ammon, C. J. and Julia, J. (2001). Application of joint receiver-function surface-wave dispersion for local structure in Eurasia, in *Proceedings of the 23rd Seismic Research Review: Worldwide Monitoring of Nuclear Explosions*, LA-UR-01-4454, Vol. 1, pp. 46–54.
- Julia, J., Ammon, C.J., Herrmann, R.B. and Correig, A.M. (2000). Joint inversion of receiver function and surface wave dispersion observations. *Geophys. J. Int.*, 143(1): 99–112.
- Julia, J., Ammon, C. J. and Nyblade, A. A. (2005). Evidence for mafic lower crust in Tanzania, East Africa, from joint inversion of receiver functions and Rayleigh wave dispersion velocities, *Geophys. J. Int.*. Blackwell Science for the Royal Astronomical Society, the *Deutsche Geophysikalische Gesellschaft* and the *European Geophysical Society*, International, International, pp. 555.
- Lawrence, J.F. and Wiens, D.A. (2004). Combined Receiver-Function and Surface Wave Phase-Velocity Inversion Using a Niching Genetic Algorithm: Application to Patagonia. *Bull. Seismol. Soc. Am.* 94: (3), 977–987.
- Ozalaybey, S., Savage, M.K., Sheehan, A.F., Louie, J.N. and Brune, J.N. (1997). Shear-wave velocity structure in the northern Basin and Range province from the combined analysis of receiver functions and surface waves. *Bull. Seismol. Soc. Am.* 87: (1): 18–199.
- Pareto, V. (1906) *Manuale di Economica Politica*, Societa Editrice Libreria. Milan; translated into English by A.S. Schwier as *Manual of Political Economy*, edited by A.S. Schwier and A.N. Page, 1971. New York: A.M. Kelley.
- Pulliam, J. and Sen, M.K. (2005). Assessing Uncertainties in Waveform Modeling of the Crust and Upper Mantle, in *Proceedings of the 27th Seismic Research Review: Ground-Based Nuclear Explosion Monitoring Technologies*, LA-UR-05-6407, Vol. 1, pp. 152–160.
- Pulliam, J., Sen, M. K. and Gangopadhyay, A. (2006). Determination of Crust and Upper Mantle Structure Beneath Africa Using a Global Optimization-Based Waveform Modeling Technique, in *Proceedings of the 28th Seismic Research Review: Ground-Based Nuclear Explosion Monitoring Technologies*, LA-UR-06-5471, Vol. 1, pp. 196–208.
- Roy, L., Sen, M. K., Stoffa, P. L., McIntosh, K. and Nakamura, Y. (2005). Joint inversion of first arrival travel time and gravity data. *J. Geophys and Eng.* 2: 277–289.

- Sen, M. K. and Stoffa, P. L. (1995). Bayesian inversion in geophysics, Union of Geodesy and Geophysics; XXI General Assembly, Boulder, CO, pp. 9.
- Shibutani, T., Sambridge, M. and Kennett, B. (1996). Genetic algorithm inversion for receiver functions with application to crust and uppermost mantle structure beneath eastern Australia. *Geophys. Res. Lett.*, 23: 1829-1832.
- Tkalcic, H. et al. (2006). A multistep approach for joint modeling of surface wave dispersion and teleseismic receiver functions: Implications for lithospheric structure of the Arabian Peninsula. *J. Geophys. Res.*, 111(B11311): 10.1029/2005JB004130.
- Zhao, L.-S. and Frohlich, C. (1996). Teleseismic body waveforms and receiver structures beneath seismic stations. *Geophys. J. Int.*, 124: 525–540.
- Zhao, L.-S., Sen, M.K., Stoffa, P. and Frohlich, C. (1996). Application of very fast simulated annealing to the determination of the crustal structure beneath Tibet. *Geophys. J. Int.* 125: 355–370.